A high-connectivity approach to a hydrolytically stable MOF for CO_2 capture from flue gas

Adrian J. Emerson, Chris S. Hawes,‡ Marc Marshall, Gregory P. Knowles, Alan L. Chaffee, Stuart R. Batten* and David R. Turner*

School of Chemistry, Monash University, Clayton, VIC 3800, Australia
E-mail: stuart.batten@monash.edu, david.turner@monash.edu
Fax: +61 3 9905 4597; Tel: +61 3 9905 6293
‡ Current address: School of Chemical and Physical Sciences, Keele University, Staffordshire, ST5 5BG, United Kingdom

Supporting Information

Table of Contents

S1. Materials and methods

All solvents, reagents, and starting materials were of reagent grade or better and were used without further purification from commercial suppliers. NMR spectra were recorded on a Bruker AVANCE400 spectrometer operating at 400 MHz for ^{1}H and 100 MHz for ^{13}C nuclei. ^{1}H NMR and ^{13}C NMR spectra were referenced against the residual solvent peak for $CDCl_3$ or 1,4-dioxane for D_2O to account for shifts due to pH influences, and all spectra are reported in ppm shifts. Low resolution mass spectroscopy was carried out using a Micromass Platform II QMS Electrospray MS instrument. Infrared spectra were recorded on an Agilent Technologies Cary 630 FTIR instrument, equipped with an attenuated total reflectance (ATR) sampler. Thermogravimetric analysis was performed on a Mettler Toledo TGA/DSC1 STARe System under an atmosphere of nitrogen and immediately heated at a rate of 2.00 °C min^{-1}. Microanalysis was performed by the Campbell Microanalytical Laboratory, University of Otago, New Zealand.

Bulk phase purity of the crystalline material (at various testing stages) was confirmed with X-ray powder diffraction patterns recorded using a Bruker D8 Focus diffractometer equipped with Cu-Kα radiation (1.5406 Å), with samples mounted on a zero-background single-crystal silicon stage. Scans were performed at room temperature in the 2θ range 5-55° and compared with predicted patterns based on low temperature single crystal data (see Fig. 3). Gas adsorption analyses were carried out using Micromeritics TriStar 3020 volumetric analyser, with samples prepared by heating (150 °C) under high vacuum overnight using a Micromeritics Vacprep 061 station. Ultrahigh purity gases were used for all analyses. Temperature control was achieved using insulated ice water (273 K), liquid nitrogen (77 K) baths, or a temperature controlled water recirculator (301 K). An Intelligent Gravimetric Analyzer (IGA-1 series) by Hiden Analytical Ltd. was used to simulate a post-combustion flue gas stream (see Fig. 4).

Synthesis of N,N″-di(methyl-4-methylbenzoate)-2,2′-diaminodiethylamine (H_3Me_2L1)

Methyl 4-formylbenzoate (3.059 g, 18.63 mmol) was dissolved in methanol (100 mL). To this solution, 2,2-diaminodiethylamine (1.00 mL, 9.26 mmol) was added and the reaction was heated under reflux for 2 hours. The reaction was then cooled in an ice bath, to which sodium borohydride (1.410 g, 37.27 mmol) was slowly added in small portions. The reaction was then allowed to stir at room temperature for 5 hours, after which addition of water resulted in the precipitation of a white solid, which was washed with water and dried to yield **H_3Me_2L1** (3.571 g, 96 %).

^{1}H NMR (400 MHz, $CDCl_3$): δ 7.99 (d, 4 H, ^{3}J = 8.0 Hz), 7.41 (d, 4 H, ^{3}J = 8.0 Hz), 3.92 (s, 6 H), 3.87 (s, 4H), 2.78 (s, 8H); *m/z* (ES+) 400.5 ($[M+H]^+$, calculated for calculated for $C_{22}H_{30}N_3O_4^+$ 400.2, 100 %); IR (ATR): 750 (m), 842 (m), 1015 (w), 1103 (m), 1278 (s), 1439 (m), 1610 (m), 1711 (s), 2803 (w), 2951 (w) cm^{-1}.

Synthesis of N,N″-di(methyl-4-methylbenzoate)-N,N′,N″-tri(ethyl acetate)-2,2′-diaminodiethylamine (Me_2Et_3L1)

H_3Me_2L1 (2.051 g, 5.13 mmol) was dissolved in acetonitrile (150 mL). To this solution, ethyl chloroacetate (1.71 mL, 15.98 mmol) and K_2CO_3 (9.687 g, 70.09 mmol) were added, and the reaction was heated under reflux for 24 hours. The solution was cooled to room temperature and the white solid was filtered from the reaction mixture. The filtrate was concentrated *in vacuo* until a pale yellow oil was obtained (1.869 g, 55 %).

^{1}H NMR (400 MHz, $CDCl_3$): δ 7.97 (d, 4H, ^{3}J = 8.0 Hz), 7.40 (d, 4H, ^{3}J = 8.0 Hz), 4.14 (m, 6H), 9.91 (s, 6H), 3.83 (s, 4H), 3.39 (s, 2H), 3.34 (s, 4H), 2.76 (bs, 8H), 1.25 (m, 9H); *m*/*z* (ES+) 658.4 ($[M+H]^+$, $C_{34}H_{48}N_3O_{10}^+$ 658.3, 10 %), 680.4 ($[M+Na]^+$, calculated for $C_{34}H_{47}N_3NaO_{10}^+$ 680.3, 100 %); IR (ATR): 750 (m), 843 (m), 1012 (w), 1105 (m), 1279 (s), 1431 (m), 1439 (m), 1611 (m), 1710 (s), 1715 (s), 2805 (bw), 2959 (bw) cm^{-1}.

Synthesis of N,N″-di(4-carboxybenzyl)-N,N′,N″-tri(acetic acid)-2,2′-diaminodiethylamine trihydrochloride ($(H_8L1)Cl_3$)

Me_2Et_3L1 (1.869 g, 2.85 mmol) was dissolved in THF (50 mL) and then added to a solution of potassium hydroxide (5.017 g) in water (100 mL). The solution was then heated under reflux for 48 hours. The reaction mixture was cooled and the THF was removed by heating *in vacuo*. 12 M hydrochloric acid was slowly added until a white precipitate formed, which was then recovered by filtration (2.015 g). The crude hydrochloride salt (1.327 g) was recrystallised from a water (12 mL) and 12 M hydrochloric acid (3 mL) solution in a vial which was then sealed inside a Teflon-lined acid digestion vessel. The vessel was heated in an oven for 36 hours at 130 °C. The mixture was filtered to yield (H_8**L1**)Cl_3 as very small colourless, clusters of block-shaped crystals (0.988 g, 52 %). Single crystal X-ray diffraction experiments were attempted on the crystalline material, however a single crystal could not be isolated from the cluster that was of a suitable quality for analysis, even with the use of synchrotron radiation. NMR experiments were inconclusive due to the solubility of the compound, as the amount of NaOD required to dissolve the compound for analysis prevented the instrument from detecting any meaningful signals in either the ^{1}H or ^{13}C spectrum.

m/*z* 546.3 ($[M+H]^+$, calculated for $C_{26}H_{32}N_3O_{10}^+$ 546.2, 100 %); IR (ATR): 770 (m), 821 (w), 1063 (w), 1102 (m), 1389 (s), 1542 (s), 1589 (s), 2913 (bw), 3378 (bw) cm^{-1}; Found C, 47.66; H, 5.26; N, 6.44, Cl, 16.25; Calculated for $[C_{26}H_{34}N_3O_{10}Cl_3]$ C, 47.68; H, 5.23; N, 6.41; Cl, 16.24.

Synthesis of poly-$[Cd_{2.5}(L1)(OH_2)]\cdot DMF\cdot 4H_2O$ (1)

$(H_8L1)Cl_3$ (11.1 mg, 16.8 μmol) was combined with 4 equivalents of cadmium(II) chloride hemipentahydrate (16.3 mg, 70.1 μmol) in a vial containing DMF (2 mL) and water (2 mL). The vial was capped and placed in a dry bath heat block at 90 °C. After 72 hours, small colourless, square-shaped crystals had formed at the bottom of the vial. Yield 5.2 mg (32 %). Phase purity was confirmed by X-ray powder diffraction (see Fig. 7). TGA showed a steady mass loss of 16 % over the temperature range 30-250 °C, which is assigned to the loss of one DMF and five water molecules (one aqua ligand and four lattice water molecules) (see Fig. S3).

IR (ATR): 733 (m), 812 (m), 1077 (s), 1343 (m), 1393 (s), 1530 (s), 1585 (s), 1601 (s), 1651 (m), 2933 (bw), 3387 (bw) cm^{-1}; Found C, 35.39; H, 4.44; N, 5.72; Calculated for $[C_{26}H_{26}N_3O_{10}Cd_{2.5}]\cdot DMF\cdot 5H_2O$ C, 35.37; H, 4.41; N, 5.69.

S2. X-Ray crystallography

Refinement and structural information is presented in Table 1. Data collection was carried out on the MX1 beamline at the Australian Synchrotron, part of ANSTO, operating at 17.4 keV (λ = 0.7108 Å) using BluIce control software.[1,2] The diffraction data was indexed and integrated using the XDS software suite,[3] and anomalous dispersion corrections for the nonstandard wavelength were made in the final refinement using Brennan and Cowan data.[4] The dataset was solved using direct methods with SHELXS[5] and refined on F^2 using all data by full matrix least-squares procedures with SHELXL-2014[6] within the OLEX-2 GUI.[7] Non-hydrogen atoms were refined with anisotropic displacement parameters, while most hydrogen atoms were included in calculated or restrained positions with isotropic displacement parameters either 1.2 or 1.5 times the isotropic equivalent of the their carrier atoms. Where appropriate, hydrogen atoms involved in hydrogen bonding interactions were located based on Fourier residuals, and appropriate distance restraints and U_{iso} dependencies were applied.

For compound **1**, significant regions of disordered electron density were detected in the Fourier difference map after the refinement of all framework atoms. No lattice solvent molecules could modelled to these sites, and the residual electron density had their contribution to the diffraction data accounted for with the SQUEEZE routine within PLATON.[8] Assignment of any lattice solvent molecules were made on the basis of calculated electron count, thermogravimetric analysis and microanalysis. The lattice solvent detected by bulk-phase methods have not been included in the crystallographic formula, and as such the values of F_{000}, density and absorption coefficients have been calculated from the crystallographically modelled atoms only. The functions minimized were $\sum w(F_o^2 - F_c^2)$, with $w = [\sigma^2(F_o^2) + aP_2 + bP]^{-1}$, where $P = [\max(F_o)^2 + 2(F_c)^2]/3$.

Analysis of the voids from SQUEEZE results in a total electron count of 536 e^- within the voids per unit cell, with a void volume of 1878 $Å^3$. There are eight formula units within the unit cell of 1, which calculates to a total solvent electron contribution of 640 e^-. While this value appears to be larger than the value calculated using SQUEEZE, the volume occupied by the calculated solvents is 1296 $Å^3$ (18 $Å^3$ per non-hydrogen atom), which appears to be a reasonable volume of solvent per void per unit cell. This amount of solvent also reasonably matches the 16 % mass loss observed in TGA, with a calculated mass of 14 % (with the remaining 2 % from the aqua ligand that is displaced during the TGA experiment).

Table S1: Crystallographic refinement details for poly-$[Cd_{2.5}(\mathbf{L1})(OH_2)]\cdot DMF\cdot 4H_2O$.

Compound reference	poly-$[Cd_{2.5}(L1)(OH_2)]\cdot$solv **(1)**
Chemical formula	$C_{52}H_{56}Cd_5N_6O_{22}$
Formula mass	1679.02
Crystal system	tetragonal
***a*/Å**	20.566(3)
***b*/Å**	20.566(3)
***c*/Å**	16.547(3)
α/°	90
β/°	90
γ/°	90
Unit cell volume/ Å^3	6999(2)
Temperature/K	100
Space group	$P4_2/n$
Z	4
ρ_{calc}***/g cm^{-3}***	1.593
μ/mm^{-1}	1.564
F(000)	3304.0
2θ range/°	3.16 to 53.05
Reflns measured	102399
Indep reflns	7266
Reflns obsd (*I* > 2σ(*I*))	4899
Data/restraints/ parameters	7266/5/392
GOOF on F^2	1.015
R_{int}	0.1755
R_1 (*I* > 2σ(*I*))	0.0518
***wR*(F^2) (*I* > 2σ(*I*))**	0.1182
R_1 (all data)	0.0901
***wR*(F^2) (all data)**	0.1357
CCDC no.	1855034

S3. Structural diagrams/description

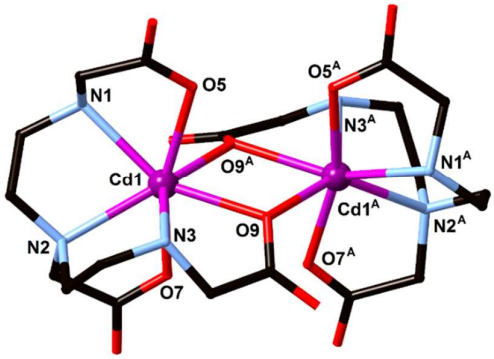

Figure S1. The coordination environment around Cd1, which involves chelation from the three amines, monodentate coordination from each acetate group and bridging from O9 to an equivalent Cd1 ion to form the dimer. The benzoic acid groups, Cd2, Cd3 and hydrogen atoms are omitted for clarity. Symmetry generated atoms: A) 3/2-x, 1/2-y, +z.

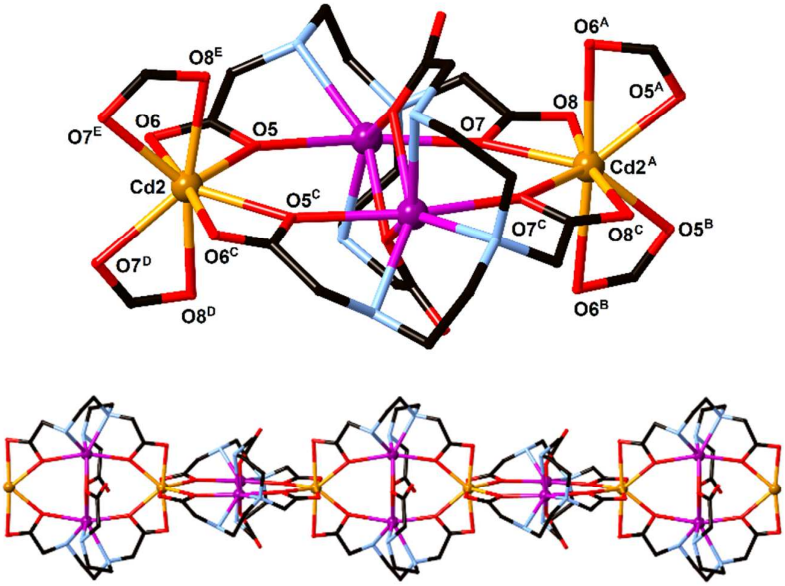

Figure S2. (Top) The Cd1 dimer is capped on either side by coordination of Cd2 *via* the O5/O6 and O7/O8 acetate groups. Symmetry generated atoms: A) 1-x, 1/2+y, -1/2+z, B) -1/2+x, 1-y, -1/2+z, C) 3/2-x, 1/2-y, 1+z, D) -1/2+x, 1-y, 1/2+z, E) 1-x, 1/2+y, 1/2+z. (Bottom) The infinite chain that is formed by Cd2 linking the Cd1 dimers, which rotates down the crystallographic 4_2 screw axis. The benzoic acid groups, Cd3 and hydrogen atoms are omitted for clarity.

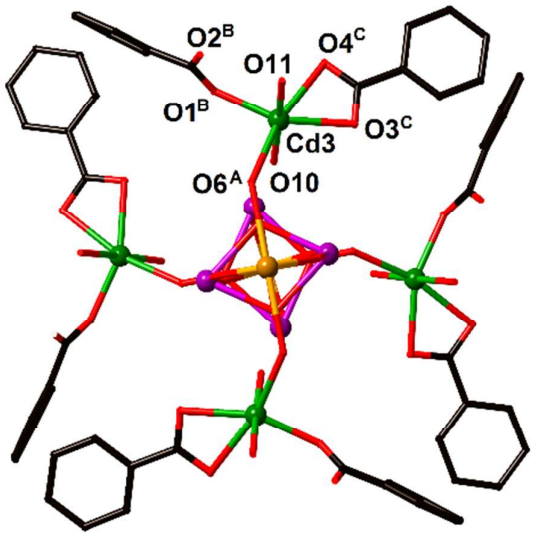

Figure S3. The coordination environment around Cd3 when viewed down the 4_2 screw axis of the infinite Cd1/Cd2 chain. The acetates O6 and O10 link Cd3 to the infinite chain while the O1/O2 and O3/O4 benzoates link each chain to neighbouring chains. Symmetry generated atoms: A) 1-x, 1/2+y, -1/2+z, B) 1+x, 1/2-y, 1/2-z, C) 1+x, 3/2-y, 1/2-z.

Cd1 (purple in Fig. 1) is seven coordinate, with 3 N-donors and 4 O-donors completing the irregular coordination environment. The N-donors consist of the three amines from the 2,2-diaminodiethylamine chelation pocket N1, N2 and N3 at distances of 2.396(2), 2.449(3) and 2.459(3) Å respectively. Three of O-donors are due to monodentate coordination by the three acetate groups off each amine O5, O7 and O9 at distances of 2.436(5), 2.333(5) and 2.363(2) Å respectively. The coordinating O9 acetate acts as a bridge to another Cd1 centre to complete the coordination environment for Cd1 at a distance of 2.277(3) Å, generating a dimer motif as shown in Fig. 2.

Cd2 (orange in Fig. 1) is eight coordinate with chelation from four acetate groups, two of which are the O5/O6 acetate group and the other two are the O7/O8 acetate group (Fig. 3). The directionality of the chelation results in Cd2 adopting a pseudo-tetrahedral geometry. The O7/O8 acetate coordinates symmetrically with Cd—O distances of 2.365(3) and 2.394(3) Å respectively, however the O5/O6 acetate coordinates asymmetrically such that the O5 distance is 2.324(3) Å and the O6 distance is 2.628(4) Å. O5 and O7 bridge Cd2 to Cd1 which results in the dimer units being linked into a one-dimensional chain, as shown in Fig. 3. The orientation of the Cd1 dimer alternates down the crystallographic 4_2 screw axis.

The six coordinate Cd3 (green in Fig. 1) is coordinated by the O6 and O10 acetates in a monodentate fashion along the edges of the one-dimensional chain, at distances of 2.309(2) and 2.248(3) Å respectively. Cd3 also coordinates to both of the benzoate groups, with monodentate coordination

from O1 at 2.181(3) Å and symmetric chelation from O3 and O4 at 2.303(3) and 2.396(2) Å. The aqua ligand O11 completes the coordination environment around Cd3 at a distance of 2.352(4) Å, while also forming a hydrogen bond to O2 with a donor-acceptor distance of 2.665(3) Å. O10 and O11 occupy axial coordination sites around Cd3, with O1, O3, O4 and O6 occupying the equatorial positions in a distorted octahedral (pseudo-trigonal bipyramidal) geometry (Fig. 4). The benzoates that coordinate to Cd3 originate from **L1** ligands from neighbouring chains, which results in the formation of the three-dimensional network.

S4. Thermogravimetric analysis

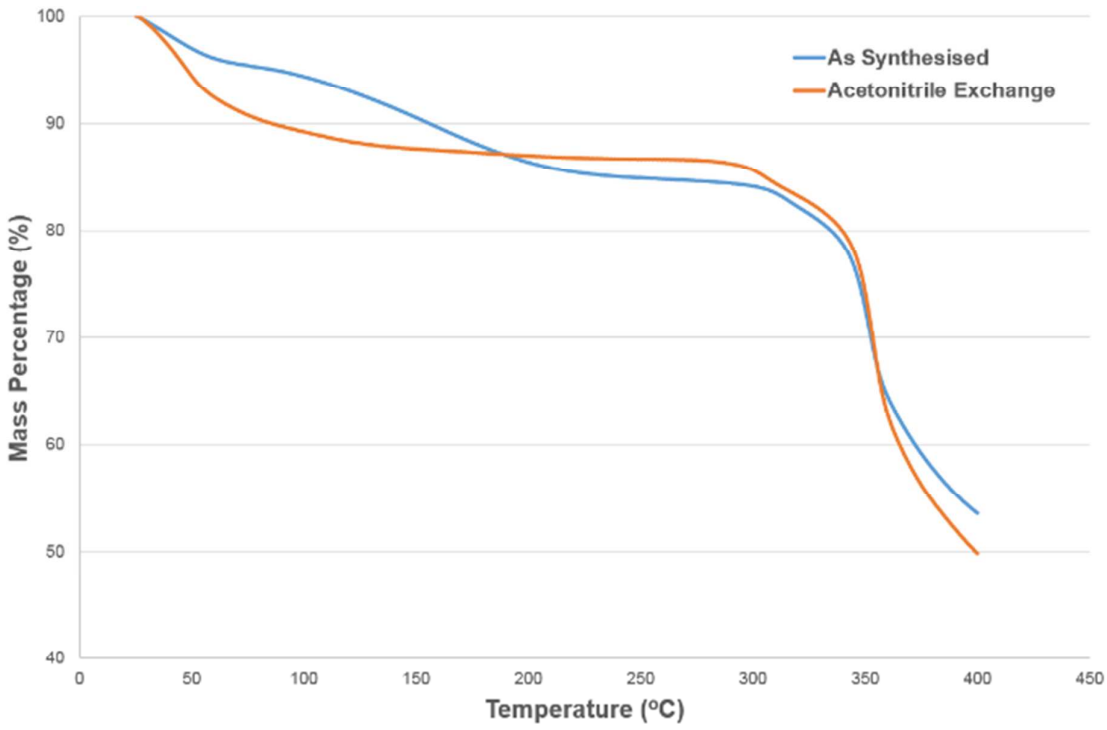

Figure S3. Thermogravimetric analysis of the as synthesised sample of **1** (blue) and the acetonitrile exchanged sample of **1** (orange).

S5. Enthalpy of adsorption

The heat of adsorption for CO_2 within complex **1** was estimated by least-squares fitting of a virial thermal adsorption equation[9,10] modelling ln(P) as a function of adsorbed CO_2. Datapoints were collected at 273K and 301K and fitted across the loading range for which datapoints were measured at both temperatures. The model function takes the form $\ln(P) = \{\ln(N) + (a_0 + a_1N + a_2N^2\ldots)/T + b\}$, with N representing the surface excess adsorption (mmol) at temperature T and a_0 and a_1 are coefficients determined through least-squares fitting. The original parameter set of 5 parameters was sequentially reduced to maximise the data:parameter ratio. The heat of adsorption at loading N is given by the relation $Q(N) = -R(a_0 + a_1N + a_2N^2)$. Optimised coefficients and parameters are given below.

Temperatures (K)	273, 301
a_0	-3380.51
a_1	88.26702
B	14.94176
R^2	0.9909
Datapoints fitted	65

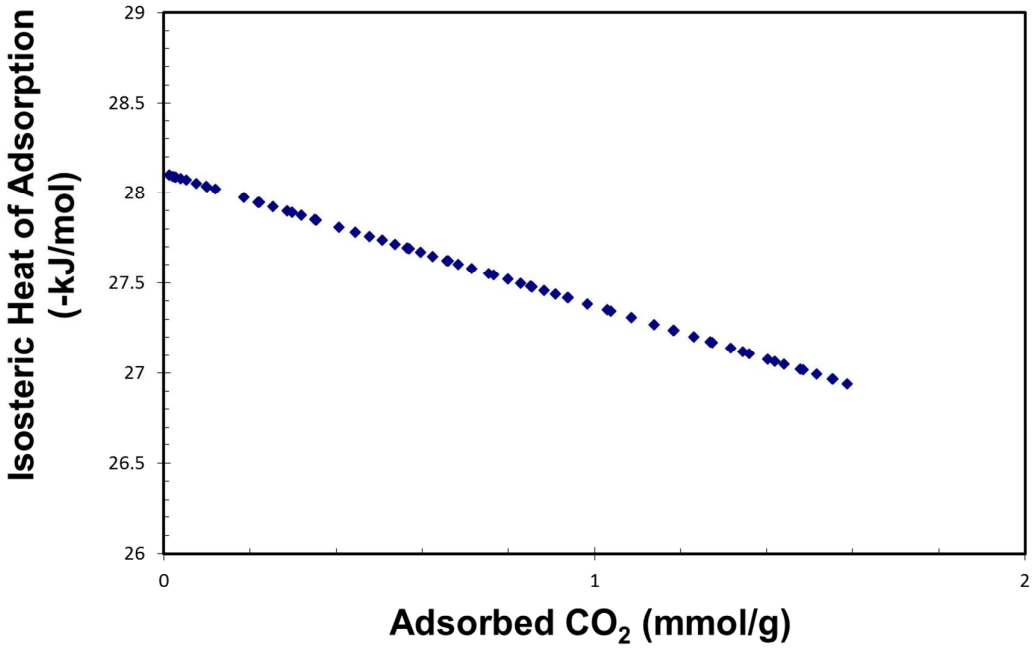

Figure S4. Calculated trace for the zero coverage enthalpy of adsorption.

References

[1] Cowieson, N.P.; Aragao, D.; Clift, M.; Ericsson, D.J.; Gee, C.; Harrop, S.J.; Mudie, N.; Panjikar, S.; Price, J.R.; Riboldi-Tunnucliffe, A.; Williamson, R.; Caradoc-Davies, T. MX1: a bending-magnet crystallography beamline serving both chemical and macromolecular crystallography communities at the Australian Synchrotron *J. Synchrotron Rad.* **2015**, *22*, 187-190.

[2] McPhillips, T.M.; McPhillips, S.E.; Chiu, H.J.; Cohen, A.M.; Deacon, A.M.; Ellis, P.J.; Garman, E.; Gonzalez, A.; Sauter, K.; Phizackerley, R.P.; Soltis, S.M.; Kuhn, P. Blu-Ice and the Distributed Control System: software for data acquisition and instrument control at macromolecular crystallography beamlines, *J. Synchrotron Rad.* **2002**, *9*, 401-406.

[3] Kabsch, W. Automatic processing of rotation diffraction data from crystals of initially unknown symmetry and cell constants, *J. Appl. Crystallogr.* **1993**, *26*, 795-800

[4] Brennan, S.; Cowan, P.L. A suite of programs for calculating X-ray absorption, reflection, and diffraction performance for a variety of materials at arbitrary wavelengths, *Rev. Sci. Instrum.* **1992**, *63*, 850-853.

[5] Sheldrick, G.M. A short history of SHELX, *Acta Crystallogr., Sect. A* **2008**, *64*, 112-122.

[6] Sheldrick, G.M. Crystal structure refinement with SHELXL, *Acta Crystallogr., Sect. C* **2015**, *71*, 3-8.

[7] Dolomanov, O.V.; Bourhis, L.J.; Gildea, R.J.; Howard, J.A.K.; Puschmann, H. OLEX2: a complete structure solution, refinement and analysis program, *J. Appl. Crystallogr.* **2009**, *42*, 339-341.

[8] Spek, A.L. PLATON SQUEEZE: a tool for the calculation of the disordered solvent contribution to the calculated structure factors, *Acta. Crystallogr., Sect. C* **2015**, *71*, 9-18.

[9] Czepirski, L.; Jagiello, Virial-type thermal equation of gas-solid adsorption, *J. Chem. Eng. Sci.* **1989**, *44*, 797-801.

[10] Tedds, S.; Walton, A.; Broom, D. P.; Book, D. Characterisation of porous hydrogen storage materials: carbons, zeolites, MOFs and PIMs, *Faraday Discuss.* **2011**, *151*, 75-94.